© 2017 IJSRSET | Volume 3 | Issue 5 | Print ISSN: 2395-1990 | Online ISSN : 2394-4099
Themed Section: Engineering and Technology

Erosion Wear Mathematical Model for WC-Co Reinforcement Hardness Distribution in Fe-Based Alloy Matrix With Evoluted Algorithms

Francisco Casesnoves MSc MD
Mechanical Engineering, Tallinn University of Technology, Computational Engineering Researcher, IEEE Individual Researcher, Estonia

ABSTRACT

The current mathematical models for erosion, corrosion, tribocorrosion and biotribology have become more complicated in current industrial manufacturing because of the number of compounds in the physical-chemical structure of the material—with special difficult-significance in alloy reinforced matrix with changes in hardness distribution. In previous contributions, an Integral-Differential, [Casesnoves, 2016], model was presented in its main characteristics and primary numerical algorithms. In this step-up the study is looked up towards the specific mathematical construction of the model, algorithms with numerical determinations and comments about comparative study related to other discrete models. An initial comparison between functional integral-differential and discrete models based on statistical distributions is overviewed. The experimental materials in this theoretical-practical research are Fe–Cr–Si–B self-fluxing alloy powder with WC-Co spherical reinforcement. Nonlinear computational optimization results, graphical nonlinear optimization, [Casesnoves, 2017], based on experimental laboratory data, are shown with additional simulations and graphical optimization techniques.

Keywords: Nonlinear Optimization, Mathematical Model, Alloy Reinforcement, Simulations, Convex Optimization.

I. INTRODUCTION AND MATHEMATICAL MODELLING METHODS

Mathematical modelling has become the most advantageous method for impact erosion wear simulations actually. Standard tribotesting requires a previous trial with computational algorithms to check the validity of the lab work that is planned to be kept on and the experimental hurdles to be sorted. In Tallinn University of Technology, the hardmetal reinforcement content for Fe-based self-fluxing alloy matrix hardfacings for use under abrasive-impact wear conditions has been extensively studied, both theoretically and experimentally.

The experimental data for this contributions is based on hardfacings with hardmetal contents of 20, 40, 60, and 80 wt% which are produced from disintegrator-milled unsorted hardmetal scrap and commercial Fe–Cr–Si–B self-fluxing alloy powder by liquid-phase sintering in vacuum.

The method that is applied to obtain graphical and computational nonlinear optimization is multiobjective optimization with L_2 Norm. This software has been designed according to mathematical modelling presented in previous contributions. Graphical optimization is developed in 3D and 2D, and numerical results are obtained through objective functions with theoretically set-constraints for better learning. The models applied for optimization are basic equations that give a general methodology overview, and these techniques are easily exported/applied on specific models for any particular erosion/corrosion/tribological study. Results are considered acceptable at this first stage and prospective research involves significant mathematical further development and improved programming software for stepping forward the investigation line.

When the simulations/optimization stage is concluded/verified, it is possible to proceed to tribotesting and begin to implement completely new/specific laboratory data and new findings when performing the experimental—by using the selected model. The theoretical final phase is to optimize the mathematical framework and to prepare for the period of final validation. In this key point, the inverse and forward methods are strictly applied, i.e., from empirical data towards the model and from theoretical simulations of the model to comparisons with lab database. To summarize, this paper sets new contributions both in mathematical-computational improvements initialized in previous international publications, and details extended nonlinear algorithms for the integral-differential erosion model [Casesnoves 2016]

II. EXPERIMENTAL DATA SET-UP ON MATHEMATICAL MODEL OBJECTIVE FUNCTION

The experimental data implemented in this model was obtained through determination of hardface hardness from lab experimental measurements. Composition of alloy-reinforced experimental samples is 70 FeCrBSi, 30 WC-Co—in total a series of 100 measurements were carried out. This research is however focused on modeling of reinforcement erosion and hardness implementation in integral-differential model [Casesnoves, 2016]. In Table 1, a few measurements are detailed, in HV units that were passed on MPa for numerical calculations. Experimental apparatus for these measurements was Universal hardness (HU) and modulus of elasticity (E) were simultaneously determined according to the standard EN/ISO 14577-02 using the universal hardness tester 2.5/TS (Zwick). The applied load and the indentation depth were respectively 50 N and 100 μm. The average values of HU and E were calculated on the basis of five measurements.

TABLE I

EXAMPLES OF EXPERIMENTAL DATA FOR MODEL DEVELOPMENT [TALLINN UNIVERSITY OF TECHNOLOGY LABORATORY,ESTONIA]		
NUMBER OF MEASUREMENT TOTAL MEASUREMENTS OF HARDFACE= 31	**HARDNESS [HV]**	
	COMMENTS Approximations without double-precision are set	
1	1653	
10	1848	
20	1936	
30	12067	
Approximate Monte-Carlo determination of average diameter of reinforcement spheres at hardface surface	3000μm	
Experimental lab data for optimization	V=40m/s erosion=3 mm^3/Kg	V=80m/s erosion =18 mm^3/Kg
Average density of reinforcement spheres/conversion factor (CF) from HV to mm^3/Kg	14.7e(-6) Kg/mm^3 CF = 9807.0	

Table 1.- Numerical values of hardface hardness from lab experimental measurements. Composition of alloy-reinforced experimental samples is 70 FeCrBSi, 30 WC-Co whose data was implemented for optimization of K wear coefficient in Eq. 1. [Tallinn University of Technology Lab].

In Fig. 1 it is shown an ultramicroscopic image of the spherical reinforcement distribution in the hardface with the matrix and binding zone images inset. This model is proper for reinforcement part whose hardness is increasing from the interface towards the spherical center of the WC-Co geometry. The physical reasons for this reasoning are, firstly, the fundamental physics laws of action-reaction, and secondly the vectorial splitting-distribution of the applied forces of the experimental pyramidal-indentor related to the micro-curvature of the reinforcement surface from the interface to the center of the spherical particle of WC-Co. In Fig. 2 the approximately radius of the spherical reinforcement is shown.

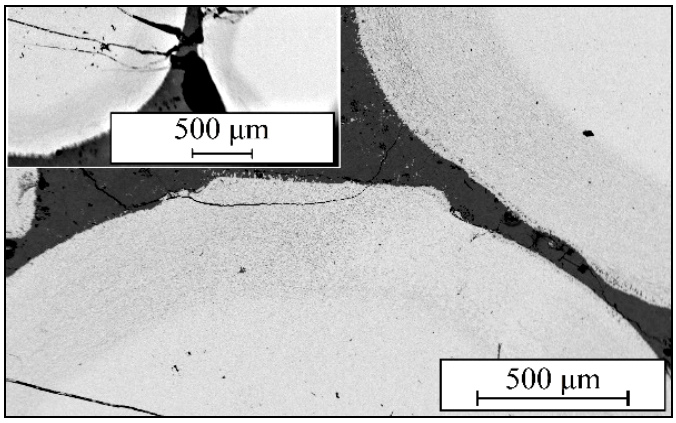

Figure 1. Experimental sample from Materials Institute lab, showing the microstructure of the studied hardfacings. Matrix and reinforcement are shrply defined, and the shadow of the interface, binding zone, is also clear.Composite hardfacing with 50 vol.% spherical WC-Co reinforcement. The numerical hardface data that was implemented in mathematical development for optimization corresponds to this kind of material, and are very easy to visually-calculate-read approximately. Microdistances proportion in image was determined by the Omnimet software accurately. Images of composite obtained with scanning electron microscope (SEM) EVO MA-15 at Tallinn University of Technology Lab.[Optical microscope Axiovert 25 (Carl Zeiss) and Buehler® Omnimet® software].

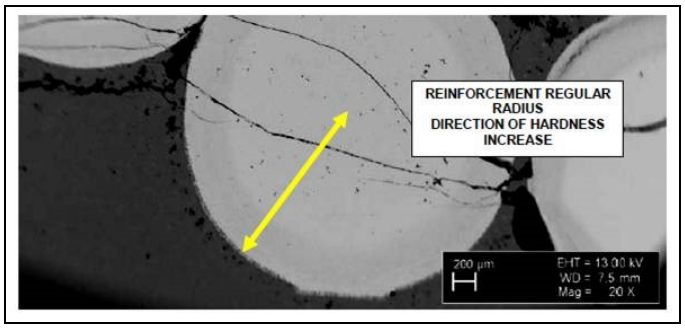

Figure 2. Enhanced, experimental sample from Tallinn University of Technology lab, showing the microstructure of the studied hardfacings. Just the same as Fig. 1, Composite hardfacing with 50 vol.% spherical WC-Co reinforcement. In this picture the approximately constant radius of the spherical surfactal-reinforcement is set inset, yellow arrows—around 6 x 200µm . This distance is used to obtain a well-implemented polynomial equation numerically.

The mathematical development of the model begins with formulation of some selected simple models, as was done in previous contributions, with the intention to explain the technique that can be used for any other equation, no matter its degree of complication. A basic erosion model form Hutchings, specifically for low impact angles is,

$$E = \frac{K\rho[V]^{2.5} f(\theta)}{H(s)} \quad ;$$

and according to optimization results with inverse determinations

$$f(\theta) \cong \cos\theta \quad ;$$

Eq. 1

where ρ is the density of the material being eroded, V is the initial particle velocity and H is the target surface hardness. K represents the fraction of material removed from the indentation as wear debris and is also known as the wear coefficient.

Before getting into nonlinear algorithms, the first step is to approximate the hardness lab data spatial-distribution along the grains of reinforcement 3D geometry. Approximations are, firstable, that the average diameter at hardface where indentation apparatus for hardness measurements act, is constant—see Table 1. Secondly, the micro-curved surface of the grains that constitutes a micro-protuberance at hardface surface, holds approximately the same curvature/symmetry for all spots of reinforcement—to set the impact hypotheses for mechanical forces distribution and energy transfer at impact instant. In fig. 3, these theoretical mechanics concepts with consequences in programming of Fig. 4 are explained.

In this model, rather lower impact angles are better considered, with consequences in cutting-wear as predominant erosion phenomena. The function f(θ) was determined with approximations according to cutting-abrasion wear lab experimental data. If the hardness is considered a continuous and derivable function, the differentiable development follows straightforward,

Direct application of chain – therorem – derivation,

$$\frac{dw}{ds}=\frac{dw}{dH}\times\frac{dH}{ds}=$$

$$=\left(K\rho\,[V]^{2.5}\cos\theta\right)\times\left(\frac{-1}{H^2(s)}\right)\times\left(\frac{dH(s)}{ds}\right);$$

integrating along all reinforcement average radius length [x 2],

$$2\int_{w_0}^{w} dw=\int_{s_0}^{s}\left(K\rho\,[V]^{2.5}\cos\theta\right)\times\left(\frac{-1}{H^2(s)}\right)\times\left(\frac{dH(s)}{ds}\right)ds;$$

however hardface has weight factors for spatial – surface distribution, [matrix, interface, reinforcement], W = ...

$$...2F_R\int_{w_0}^{w} dw=\int_{s_0}^{s}\left(K\rho\,[V]^{2.5}\cos\theta\right)\times\left(\frac{-1}{H^2(s)}\right)\times\left(\frac{dH(s)}{ds}\right)ds;$$

with F_R as weight – surfactal factor for reinforcement;

Eq. 2

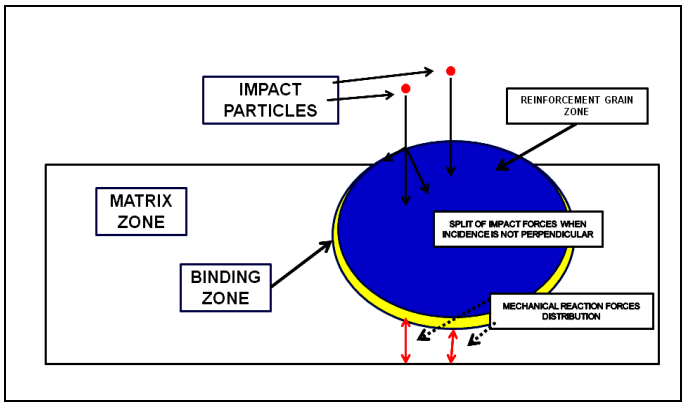

Figure 3. Theoretical Mechanics application of action-reaction theorem and vectorial forces distribution to prove the hypothesis of the hardness spatial-distribution along grain-reinforcement surfactal-hardface. Hardness of reinforcement surface results of higher magnitude measurement for perpendicular particle incidence and action-reaction at lower part of sample, with perpendicular direction in lower-content of matrix material zone also.

According to Fig. 3 forces impact forces and hardness distribution,the function H(s) has been determined by using the laboratory data in a programming polynomial least-squares fitting whose result is,

H(s)= 1.0e+003 x [0.0014 S^2 + (-0.0025) S + 1.8671 ;

Residual (error) = normr: 102.5165

Eq. 3

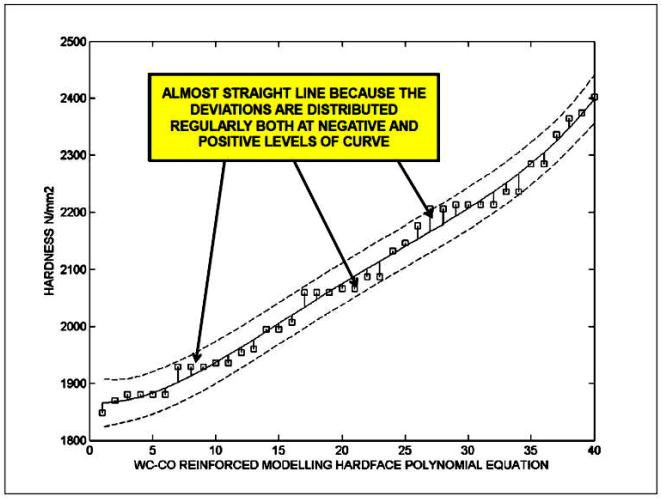

Figure 4. Numerical polynomial software least-squares programming results for reinforcement to obtain the Hardness continuous function. The polynomial fitting is considered acceptable with low residual, and sharp resemblance to an straight line.

Other type of formulation-model, simpler, that has been simulated/optimized in previous publications is,

$$W=\frac{K\rho U^2}{2H};$$

Eq. 4

where ρ is the density of the material being eroded, U is the initial particle velocity and H is the target surface hardness—this equation is simpler compared to Eq. 1. K

represents the fraction of material removed from the indentation as wear debris and is also known as the wear coefficient. In this contribution the computational work is exclusively concentrated on model of Eq. 1.

This is an example about how the integral-differential model can be obtained, provided now that the impact

velocity is not constant as happens with the hardness, and also the density of the material is not regular (constant) along the hardface, so the algorithm increases in complexity and the differential is,

Setting the total differential theorem,

$$dw = \frac{\partial w}{\partial H}dH + \frac{\partial w}{\partial v}dv + \frac{\partial w}{\partial \rho}d\rho =$$

$$= \left(K\rho v^2\right) \times \left(\frac{-1}{2H^2(s)}\right) \times \frac{dH}{ds} \times ds +$$

$$+ \left(\frac{K\rho}{2H}\right) \times (2v)dv + \left(\frac{Kv^2}{2H}\right) \times \ d\rho =$$

integrating along all reinforcement spots average radius length, and using weight factor for reinforcement, W = ...

$$...2xF_R \int_{w_0}^{w} dw = \int_{s_0}^{s} \left(K\rho v^2\right) \times \left(\frac{-1}{2H^2(s)}\right) \times \left(\frac{dH(s)}{ds}\right) ds + \ldots$$

$$\cdots + \int_{v_0}^{v} \left(\frac{K\rho}{H}\right) \times (v) \times dv + \int_{\rho_0}^{\rho} \left(\frac{Kv^2}{2H}\right) \times \ d\rho \, ;$$

with the complete erosion to be determined in all weight factors,

OPTIMIZATION PARAMETERS IN SIMULATIONS AND BOUNDARIES FOR OBJECTIVE FUNCTION (OF)		
Experimental lab data for optimization	V=40m/s erosion=3 mm^3/Kg	
Material Composition [wt.%]	Reinforcement shape	
70 FeCrBSi, 30 WC-Co	Spherical	
50 FeCrBSi, 50 WC-Co	Spherical	
Average density of reinforcement spheres/conversion factor (CF) from HV to mm^3/Kg	14.7e(-6) Kg/mm^3 CF = 9807.0	
SETTING UPPER AND LOWER BOUNDARIES AND PARAMETERS		
K /V ; boundaries/velocities, 1,2	[0.0 , 200.0] ; 1/40m/s ;2/ 80 m/s	
Alpha boundaries for cosθ, 1,2 intervals	1, [0.0 , 1.0]	2, [0.3420 , 1.0]

Eq. 5

Therefore, this equation defines, as an instance, how the current variable hardfaces of alloy with at least one reinforcement could be analyzed in terms of erosion provided the geometry for every compound is well-defined at least at high-micro level. In the subsequent section the optimization algorithm for Eq. 1 and results are presented.

III. COMPUTATIONAL AND NUMERICAL-PROGRAMMING RESULTS

The first step is to define sharply the Objective Function (OF) to be applied. It is a Least-Squares Multiobjective Optimization Function with L_2 norm. Therefore, for Eq. 1, the OF with constraints reads,

minimize,

$$F(\vec{x}) = \sum_{i=1}^{i=N} \left\| H_i - f(\vec{x}) \right\|^2 \; ; \text{subject to,}$$

$$a_1 \le K \le a_2 \; ;$$

$$b_1 \le \alpha \le b_2 \; ; \quad \text{with,}$$

$$f(\vec{x}) = \frac{K\rho \times [v]^{2.5} \cos\theta}{2W} \; ;$$

determination of optimal impact angle and wear constant within intervals, $[a_1 \, , a_2]$ and $[b_1 \, , \, b_2]$;

Eq. 6

TABLE II

Table 2.-Numerical data that was implemented for nonlinear optimization of Eq. 6 . Experimental values, impact velocity, material density, and all parameters implemented are from laboratory measurements results. The boundaries are detailed in closed intervals for k and sine of impact angle.

The optimization carried out is precise in the sense that what is sought is to get examples of setting intervals with upper and lower bounds in the model—see

discussion of results in this section and figures. Therefore, the objective is to take off computational-numerical consequences both from the data, graphs, and surfactal optimization 3D plots. For the numerical results the constraints of Eq. 6 are applied. The experimental data that was implemented for the reinforcement hardness of this model was detailed in Table 1. Table 2 shows the programming implementation data. In Table 3 the results of algorithm of Eq. 6 is presented. Multiobjective Optimization with 2 variables is rather more complicated, although was well determined by the subroutine specifically developed.

TABLE III

Table 3.-Results that were obtained from nonlinear optimization of Eq. 6 . The reading of this table has the notation corresponding to Tables 1 and 2.

In the following a number of optimization software graphical results are put forward with special interest in accuracy/clarity of images and data details at inset of pictures. Comments about the running time and characteristics of programming are added.

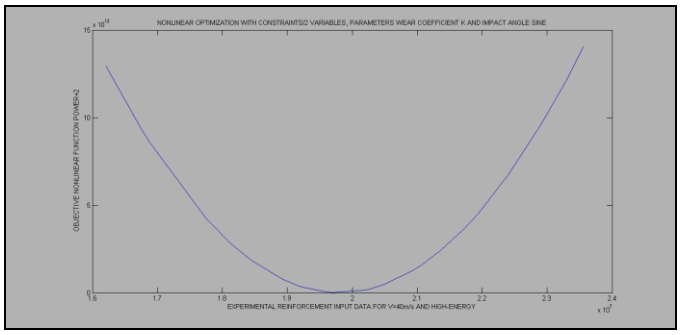

Figure 5. Objective function (OF) nonlinear optimization without constraints according to Table 3, first value [1/1/163.2485]. Results for Table 1 settings and equation model of Eq. 1. The impact velocity is 40m/s. Results are acceptable with a sharp Minimum precisely determined/bounded and running time is lower than a second.

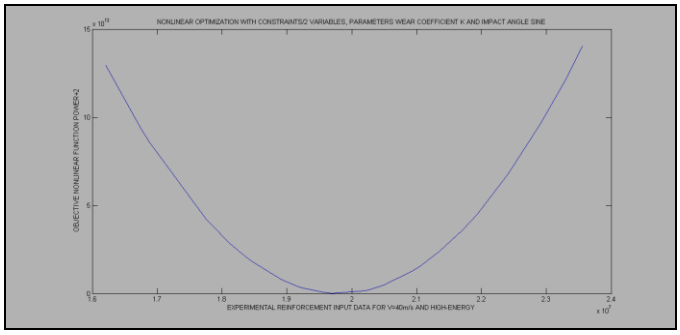

Figure 6. Objective function (OF) nonlinear optimization without constraints according to Table 3, second value [1/1/156.2399]. Results for Table 1 settings and equation model of Eq. 1. The impact velocity is 40m/s. Results are acceptable with a sharp Minimum precisely determined/bounded and running time is lower than a second.

COMPUTATIONAL SIMULATIONS-OPTIMIZATION RESULTS (MULTIOBJECTIVE OPTIMIZATION)		
Velocity/Impact Angle Boundary/Optimal K	Search Point/Residual	Optimal Angle [arcos(θ)]
1/1/163.2485	[70.0 , 0.2] /1.3862e+7	0.7738
1/1/156.2399	[40.0 , 0.3] /1.3862e+7	0.8085
1/2/152.2804	[60.0 , 0.5] /1.3862e+7	0.8296
1/2/158.9514	[80.0 , 0.4] /1.3862e+7	0.7984
2/1/89.9277	[60.0 , 0.2] /1.3862e+7	0.3725
2/1/68.4812	[70.0 , 0.4] /1.3862e+7	0.4892
2/2/62.0237	[50.0 , 0.5] /1.3862e+7	0.5401
2/2/65.5409	[100.0 , 0.6] /1.3862e+7	0.5111
COMMENTS Acceptable, (single precision), but variable results for optimization in two variables, low residual of OF minima, and optimal angles approximated to experimental data determined at laboratory		

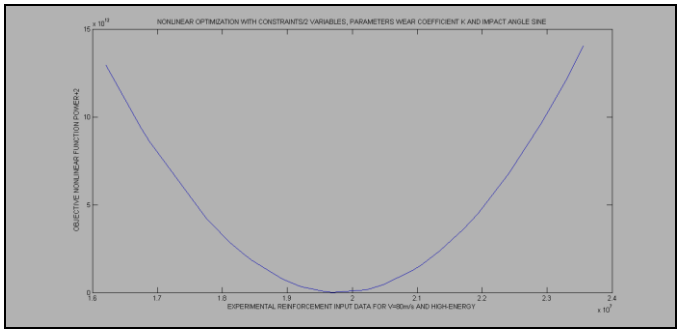

Figure 7. Objective function (OF) nonlinear optimization without constraints according to Table 3, eight value [2/2/65.5409]. Results for Table 1 settings and equation model of Eq. 1. The impact velocity is 80m/s. Results are acceptable with a sharp Minimum precisely determined/bounded and running time is lower than a second.

The graphical-surfactal optimization/simulation is shown in the following Fig. 8 to summarize the results of the research. It was programmed for the model of Eq. 1 and OF of Eq. 6 without constraints. In this Fig. 8, it is seen the model values for an interval of K and angles of impact expressed in cos(θ) values. In Appendix 1, the surfactal-simulation is detailed in different angle and higher image.

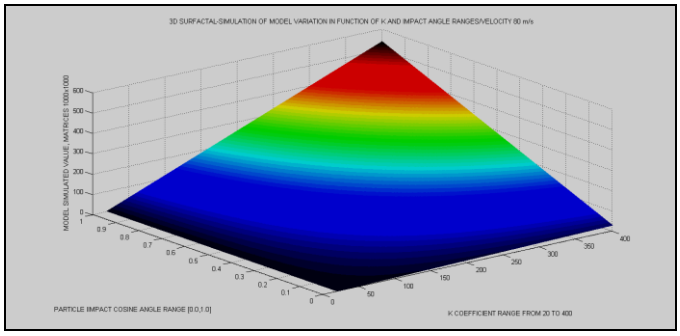

Figure 8. 3D surfactal simulation results for Table 5 and Eq. 1 without constraints. The impact velocity is 80m/s. Range of angles for cosine of impact angle are [0.0,1.0]. Range of K wear coefficient is [20.0,400.0]. Results corroborate the Tables 2,3 numerical data. That is, a global maximum is totally well-defined, and there are several local minima according to boundary-intervals. Matrices of imaging are 1000x1000. The designed software runs in 2 seconds for complete image.

To summarize, this section has presented the method to perform a constrained/unconstrained nonlinear optimization of an erosion model in two variables. Graphical optimization was added as a proof of complementary usage. The numerical results show coherence and realistic significance.

IV. DISCUSSIONS AND CONCLUSIONS

The mathematical model for abrasive erosion of Fe-based alloy with WC-Co reinforcement was developed in improved algorithms, computational software and simulations. Results can be considered acceptable since the optimization programming, graphical optimization, and imaging sharp determinations are correct. The method of setting boundaries for impact angle values according to cutting-wear experimental data has presented acceptable performance. This approach was done with realistic data from sufficient experimental measurements of hardness. A number of improvements will be subject of further publications, with extension to large-scale erosion, corrosion, tribocorrosion and biotribological models models. What was carried out in this contribution was the proof of the algorithm functionality, and its capability to get further evoloted improvements. The implementation of the laboratory experimental data into those algorithms has given a clear demonstration of integral-differential model development for the next generation of tribology types in the future.

V. ACKNOWLEDGEMENTS AND SCIENTIFIC ETHICS STANDARDS

TUT is gratefully acknowledged for all the facilities for research. This study was carried out, and their contents are done according to the European Union Technology and Science Ethics. Reference, 'European Textbook on Ethics in Research'. European Commission, Directorate-General for Research. Unit L3. Governance and Ethics. European Research Area. Science and Society. EUR 24452 EN. This research was completely done by the authors, the software, calculations, images, mathematical propositions and statements, reference citations, and text is original for the authors. This article contains also unique numerical data and special new-improved images. When anything is taken from a source, it is adequately recognized. Ideas from previous publications were emphasized due to a clarification aim.

VI. REFERENCES

[1] Abramobitz, Stegun. Handbook of Mathematical Functions. Applied Mathematics Series. 55.1972.

[2] Casesnoves F, Suzenkov A. Mathematical Models in Biotribology with 2D-3D Erosion Integral-Differential Model and Computational-Optimization/Simulation Programming. International Journal of Scientific Research in Computer Science, Engineering and Information Technology. 2017 IJSRCSEIT | Volume 2 | Issue 3 | ISSN : 2456-3307.

[3] Balamanikandasuthan, K., Arun, K., Sharath Sekar Palam (2015). Design and fabrication of erosion protection shield for boiler tubes and its analysis. International Journal of Mechanical and Materials Engineering, 1, 1, 39–52.

[4] A Surzhenkov, M Viljus, T Simson, R Tarbe, M Saarna, F Casesnoves. Wear resistance and mechanisms of composite hardfacings atabrasive impact erosion wear. IOP Conf. Series: Journal of Physics: Conf. Series 843 (2017) 012060 doi :10.1088/1742-6596/843/1/012060.

[5] I. Hussainova, On micromechanical problems of erosive wear of particle reinforcement composites, Proc. Estonian Acad. Sci. Eng. 11 (2005) 46-58.

[6] P. Kulu, R. Tarbe, A. Zikin, H. Sarjas, A. Surženkov, Abrasive wear resistance of recycled hardmetal reinforced thick coating, Key Eng. Mat. 527 (2013) 185-190.

[7] T. Simson, P. Kulu, A. Surženkov, R. Tarbe, M. Viljus, M. Tarraste, D. Goljandin, Optimization of reinforcement content of powder metallurgy hardfacings in abrasive wear conditions, P. Est. Acad. Sci. 65 (2016) 90-96.

[8] A. Surzhenkov, R. Tarbe, M. Tarraste, T. Simson, M. Viljus, P. Kulu, Optimization of hardmetal reinforcement content in Fe-based hardfacings for abrasive-impact wear conditions, Proc. Eur. Conf. Heat Treat. 2016 and 3rd Int. Conf. Heat Treat. Surf. Eng. Automotive Applications, 11–13 May 2016, Prague, Czech Republic.

[9] Kleis, I, Kulu, P. Solid Particle Erosion. Springer. 2008.

[10] Chen Q, Li D. Computer simulation of solid-particle erosion of composite materials. Wear 255 (2003) 78–84.

[11] Antonov, Renno, and collaborators. Effect of oxidation on erosive wear behavior of boiler steels.

[12] Irina Hussainova Jakob Kubarsepp Igor Shcheglov. Investigation of impact of solid particles against hardmetal and cermet targets. Tribology International 32 (1999) 337–344.

[13] Hussainova, Jakob Kubarsepp, Juri Pirso. Mechanical properties and features of erosion of cermets.

[14] Crocker, L. A review of current methods for modeling erosive wear. NPL Report. 2011.

[15] Luenberger, G D. Linear and Nonlinear Programming. Fourth Edition.Springer.2008.

[16] Casesnoves, F. 'A Monte-Carlo Optimization method for the movement analysis of pseudo-rigid bodies'. 10th SIAM Conference in Geometric Design and Computing, Texas, San Antonio, USA. Contributed Talk. November 2007.

[17] Casesnoves, F. 'Applied Inverse Methods for Deformable Solid Dynamics/Kinematics in Numerical Reuleaux Method (NRM)'. International Journal of Numerical Methods and applications. volume 9(2) 2013 .Pages 109-131. Peer-Reviewed International Mathematical/Computation Journal Article. print/Online.http://www.pphmj.com/abstract/7688 .htm. This article is specially innovative in Inverse Problems applications for deformable solids kinematics/dynamics, further publications are included in United States Congress Library.

[18] Woytowitz ,P, Richman R. Modeling of damage from multiple impacts by spherical particles. Wear 233–235 .999. 120–133.

[19] Liao H, Normand B, Coddet C. Influence of coating microstructure on the abrasive wear resistance of WC/Co cermet coatings. Surface and Coatings Technology 124 (2000) 235–242.

[20] 'European Textbook on Ethics in Research'. European Commission, Directorate-General for Research. Unit L3. Governance and Ethics. European Research Area. Science and Society. EUR 24452 EN.

[21] Casesnoves, Antonov, Kulu. Mathematical Models for Erosion and Corrosion in Power Plants. A Review of Applicable Modelling Optimization Techniques. 2016// 57th International Scientific Conference on Power and

Electrical Engineering of Riga Technical University (RTUCON). 2016.
[22] Casesnoves, F. Applied Inverse Methods for Optimal Geometrical-Mechanical Deformation of Lumbar artificial Disks/Implants with Numerical Reuleaux Method. 2D Comparative Simulations and Formulation. Computer Science Applications. Volume 2, Number 4, pp. 1-10. www.ethanpublishing.com. This article is registered as Numerical Reuleaux Method original original/published by Francisco Casesnoves in Philadelphia 2015 in United States Congress Library.

APPENDIX I

Surfactal simulation, [Casesnoves, 2017], of Fig. 8 in different angle with matrices-programmed for 100x100.